

# A field-portable instrument for mapping the micro-environment within grass canopies

J. SILVERTOWN, S. D. PRINCE\* and  
B. A. SMITH

*Biology Department, Open University, Walton  
Hall, Milton Keynes MK7 6AA, UK and \*School  
of Biological Sciences, Queen Mary College, Mile  
End Road, London E1 4NS, UK*

**Abstract.** A battery-operated field-portable instrument designed to measure the ratio of red/infra-red (R/IR) light beneath grassland canopies on a micro-scale is described. Because the ratio is correlated with leaf area index, a grid of ratio measurements may be used to map the location and size of canopy gaps. These are potential entry points into the vegetation for new individuals and for new species of plants. Measurements are made with a 1.5 mm diameter fibre optic probe which scans beneath the canopy under the control of a portable micro-computer. Data are stored on magnetic tape and processed by mainframe computer to produce contour maps of R/IR ratio.

*Key-words:* Canopy gaps, fibre-optic, light, grassland, micro-environment, microcomputer

## Introduction

In most kinds of vegetation where the Leaf Area Index is greater than unity, new individuals are only able to grow where there are gaps in the canopy and these form entry-points for new plant genotypes and new species. This is particularly obvious in forests where gaps can be viewed from beneath by the human observer but it is also true of grasslands where direct observation from beneath is not possible (e.g. Fenner, 1978; Silvertown, 1981; Silvertown & Wilkin, 1983; Wells & Haggard, 1984). Although forest gaps are easy to observe, their physical scale and the long turnover-time of tree populations makes experimental manipulation with adequate replication difficult. Populations of grassland species have rapid turnover times and grassland gaps are small in size and therefore easy to manipulate. The only drawback is that their small size makes grassland gaps

difficult to observe and measure quantitatively. The instrument described here is designed to overcome this problem and make grassland vegetation a tractable experimental system for the investigation of the role of disturbance in plant population dynamics and community structure.

## Description of the instrument

The instrument is designed to map the fluence rate under vegetation in the field, with as little disturbance to plants as possible, at two broad, non-overlapping wavebands in the red (R) and near infra-red (IR). There is a close relationship between R/IR and Leaf Area Index (Jordan, 1969; Frankland & Poo, 1980) so that a quantitative picture of the distribution of gaps, or conversely of the distribution of vegetation cover, is obtained from an R/IR map. We emphasize that we are using measurements of R/IR only as a means to the end of mapping gaps, *not* only because of its acknowledged importance as an environmental variable in itself.

Readings are taken at points in a grid of sampling locations in a plane of dimensions up to 25 cm × 30 cm, beneath the canopy. Measurements are made automatically by the instrument which is controlled by a microcomputer. The instrument is battery-powered and field-portable and consists of five parts:

- 1 A fibre-optic *probe* attached to –
- 2 A dual-wavelength *detector* which produces an analogue output.
- 3 A mechanical *scanning arm* driven by stepper motors which allow the probe to be moved to any location within a horizontal plane.
- 4 A measurement and control unit (*MCU*) which converts the analogue output of the detector to a digital signal and which controls the movement of the scanning arm. The MCU also incorporates a rechargeable battery which powers the arm and the MCU itself.

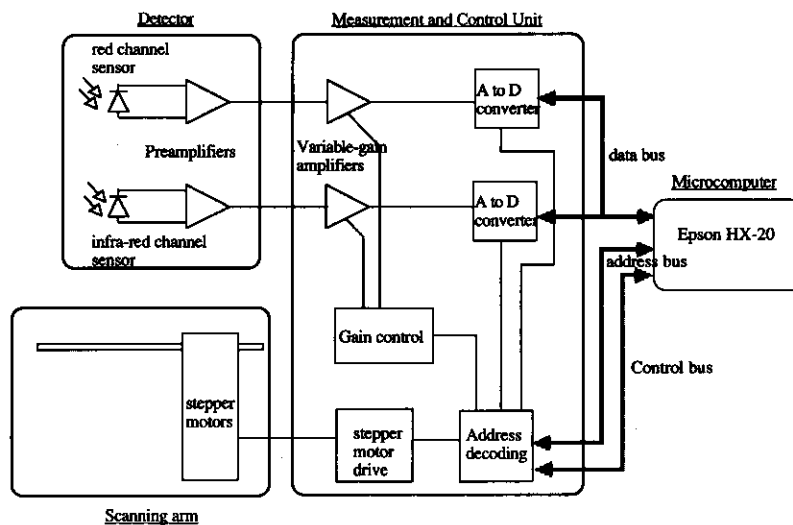


Fig. 1. Block diagram of the instrument showing its major components and their interconnections. The fibre-optic probe (not shown) is attached to the scanning arm by a clamp and transmits light to the detectors through a 'Y' junction.

- 5 A battery-powered microcomputer (Epson HX 20) interfaced with the MCU and running a programme called SENSOR which is used to input coordinates for the movement of the scanning arm, to trigger readings at programmed positions, to store digital data on tape and to perform other functions described in more detail below.

Parts 2 and 3 are contained in an acrylic box with a horizontal slit running along the length of each side to accommodate the movement of the probe; parts 4 & 5 are housed in a moulded polypropylene case with a clear acrylic lid. Fig. 1 shows the arrangement of the parts of the instrument and their interconnections.

#### Probe

The probe is a 1.5 mm diameter, polymer, fibre-optic waveguide (Crofon<sup>TM</sup>) cut at one end to form a smooth surface, 45° to the axis of the fibre. A gold mirror is formed on this surface by evaporation and is coated on the back with black enamel paint. The waveguide is inserted in a 26 cm long stainless steel tube 2.05 mm in external diameter, with its mirrored end located beneath an aperture 1.5 mm from the distal end of the tube which is sealed with epoxy resin. The other end of the tube is attached to the end of the scanning arm by an adjustable clamp and the tail of the fibre emerging from the tube is clad in opaque black plastic. The tail of the probe forms a 74 cm long flexible link to the detector.

#### Detector

At the detector, the waveguide mates through a removeable coupling with the stem of a 'Y' junction which splits the signal into two. One arm of the 'Y' junction terminates in a silicon photodiode (type BPX 65, stock no. 309-307 from R.S. Components, Corby, U.K.) covered with a red filter (Calflex) and the other in a photodiode covered with an infra-red filter (Kodak Wratten 88A). Pre-amplifiers in the detector circuit amplify the output of the photodiodes which passes through a low-pass R-C filter to reduce noise and is transmitted to the MCU by a screened lead. The detector circuit includes passive photodiodes blacked-out and wired to provide compensation for drift caused by changes in ambient temperature in the field. Photodiode dark currents are measured and compensated for in a subroutine of SENSOR (Fig. 2).

Auto-ranging of the instrument is carried out in a board in the MCU (see Fig. 1). Switching between ranges on this board is controlled by the microcomputer software (Fig. 2). Six gain ranges are used to cover a 1000-fold range in fluence rate.

#### Scanning arm

The carriage and arm are driven by two 4-phase stepper motors. The arm has a reach of 25 cm × 30 cm which enables the probe to be moved to any location within this area and to be positioned with an accuracy of 1 mm. Measurements may be taken automatically at points on any rectangular grid by

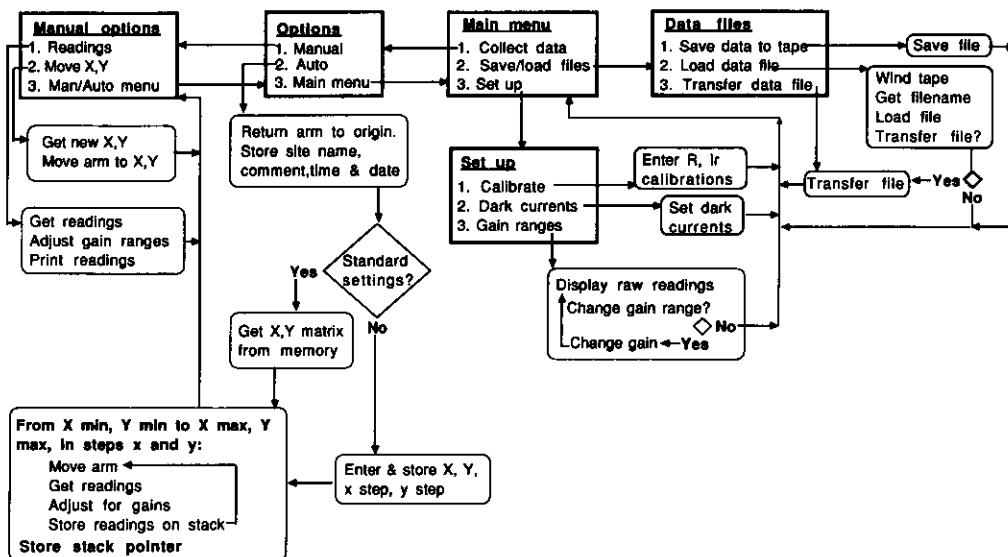


Fig. 2. Flow chart for the control programme SENSOR.

specifying (in mm) the minimum ( $X_{\min}$ ,  $Y_{\min}$ ) and the maximum ( $X_{\max}$ ,  $Y_{\max}$ ) coordinates of the grid and the interval between readings ( $x_{\text{step}}$ ,  $y_{\text{step}}$ ) in the  $X$  and  $Y$  directions. These parameters are keyed in to the microcomputer before readings begin or default values selected on a previous occasion may be used (Fig. 2). The arm begins by moving the tip of the probe to the top right hand corner of the grid, located at  $x_{\min}$   $y_{\max}$ . The arm then withdraws the probe from the vegetation, stopping every  $y_{\text{step}}$  to take a reading. By taking measurements as the probe withdraws, disturbance to the vegetation is minimized. When the probe reaches  $Y_{\min}$  it is moved a distance  $x_{\text{step}}$  along the  $X$  axis of the grid before it moves to  $Y_{\max}$  again. The cycle is repeated until the probe takes its last reading at  $X_{\max}$ ,  $Y_{\min}$ . Limit switches prevent the arm moving outside the predetermined limits of 25 cm  $\times$  30 cm and allow the position of the arm to be returned to the origin when desired. The speed of the stepper motors and their gearing limit the speed of operation of the instrument in the field. At present 676 readings take 21 min to execute in the field, though we are hoping to improve considerably on this in the near future.

#### Measurement and Control Unit

This contains a measurement board (A/D converters, variable gain amplifiers) and an interface and control board for the stepper motors and interfaces for the microcomputer and scanning

arm. The unit is powered by a rechargeable 12 v, 9.5 Ah sealed gel lead-acid battery which is mounted in the case with a trickle charger for convenient recharging in the laboratory.

#### Microcomputer and software

An Epson HX20 microcomputer is used with an internal micro-cassette tape drive and micro-printer. It is powered by its own rechargeable battery. The memory expansion port is used as an interface with the MCU and this limits all activities in the computer to the standard 16K capacity of the machine. About 8K is taken up by software, control and communications. The rest of the available RAM is used for temporary data storage. Seven hundred and twenty pairs of readings with associated positional information and a 50-character comment can be stored before it is necessary to off-load data to tape. A micro-cassette tape holds six files of this size. A flow chart for the programme SENSOR which controls the operations of the instrument is shown in Fig. 2. It is written in BASIC with some machine code routines. A version of the instrument incorporating a Husky Hawk microcomputer is currently being developed.

#### Calibration and sensor characteristics

The instrument autoranges to cope with fluence rates between  $2 \mu\text{mol m}^{-2} \text{s}^{-1}$  and  $1000 \mu\text{mol m}^{-2} \text{s}^{-1}$ . The response of the instrument is linear within this range, the limits of which can be

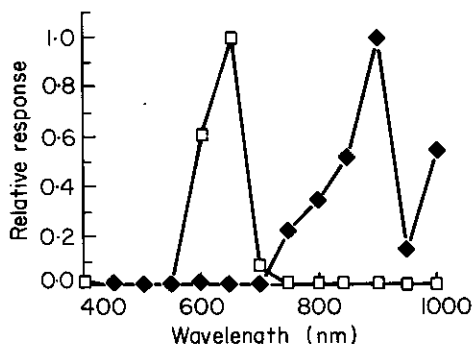


Fig. 3. Spectral response of the instrument in the red and infra-red channels.

adjusted by changing the value of feedback resistors in the amplifier circuits of the detector. Linearity of response was tested by calibration against a Li-Cor quantum radiometer (LI 185B) with a LI 190SB quantum sensor using neutral-density filters to attenuate the fluence rate of natural daylight.

The normalized spectral response of the sensor and filters is shown in Fig. 3. This spectrum is a composite calculated from the individual spectral characteristics of the optic fibre, the optical filters and the photodiodes. The two channels record across relatively broad, but non-overlapping, wavelength bands in the red and near infra-red. Peak sensitivity occurs at 650 nm in the red channel and at 900 nm in the infra-red. These characteristics give a higher signal/noise ratio with the use of fibre optics than can be obtained using 10 nm bandwidth filters at 660 nm & 730 nm as instruments designed for a different purpose have done (Woodward, 1983). Fluence rates measured by our sensors correlate with changes in daylight R/IR caused by vegetation (see below).

The optical properties of the tip of the fibre-optic probe have been designed to enable approximately point-readings to be made. Polar plots of light sensitivity versus angle of incidence in Fig. 4 show that the instrument receives light from a narrow cone of about 30° angle. For the particular probe shown in the figure the axis of the cone is not quite perpendicular to the axis of the fibre but given the small size of the tip itself (1.5 mm) this is not regarded as important. Nevertheless, we hope that better manufacturing techniques may improve this.

### Sample results

For demonstration purposes we used the instrument to map a 16 cm × 26 cm box of two-month old

*Festuca rubra* L. cut into a gradient in turf height. Readings in natural daylight were taken at a total of 442 points located at one cm intervals. Data were transferred from the Epson HX20 via an RS232 interface to a BBC Master microcomputer and from there to a mainframe Digital Equipment Corp. VAX. A contour map of R/IR ratios was drawn from the R/IR ratio values by the UNIRAS package running on the VAX (Fig. 5)

A mainframe computer programme has been written for quantifying the number and size of areas ('gaps') within a map that have a R/IR ratio above any specified value. Programmes for quantifying changes between successive contour maps taken from the same sites and for correlating seedling distribution with R/IR maps are also being developed (details available from the authors).

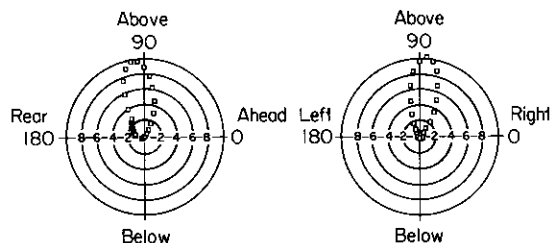
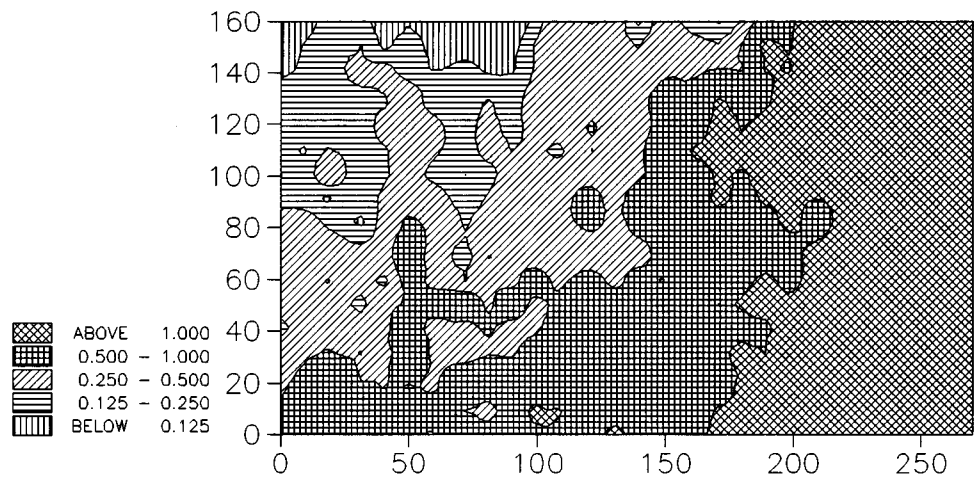


Fig. 4. Polar plots of light sensitivity, shown on a relative scale along the radii, versus angle of incidence for the fibre-optic probe described in the text. (a) Probe aligned left-to-right with its axis in the plane of the page; (b) probe aligned with its axis perpendicular to the plane of the page.

### Discussion

The evidence that seed germination, seedling fate and plant development are correlated with plant cover on a local scale in temperate grasslands is overwhelming (e.g. Gross & Werner, 1982; Silvertown & Wilkin, 1983; Watt, 1987; McConnaughay & Bazzaz, 1987; Deregibus *et al.*, 1985). Some of these effects of plant cover are a direct effect of radiation quality (Frankland, 1980) but the micro-environment beneath a canopy and in a gap also differ in other ways, such as the amplitude of temperature fluctuations which is known to influence seed germination (Thompson, Grime & Mason, 1977). Although our instrument uses a measure of radiation quality to detect gaps it is necessary to emphasize that it is not intended to measure either absolute fluence rates or some



**Fig. 5.** A contour map of R/IR ratios for a turf of *Festuca rubra* cut into a two-dimensional gradient of vegetation height from a maximum in the top left hand corner (6 cm high) to a minimum (0 cm high) at bottom right. The 160 mm × 260 mm area of turf was scanned in a grid with one reading taken every 10 mm.

specific ratio of wavelengths (Homes & Smith, 1977) but simply to provide us with a variable which correlates with spatial variation in vegetation cover (Fig. 5). Once this correlation has been achieved it becomes possible to map gaps and therefore to follow their appearance, colonization and disappearance and, so-to-speak, to study their demography. The sensor of this instrument has been miniaturized to a scale relevant to seeds and seedlings which are the most vulnerable stages of the plant life-cycle. Future work using the instrument described will report upon the correlation between gap demography and plant demography. Modifications to the instrument could allow the investigator to compare PAR above and below the grassland canopy and we are intending to develop the instrument so that dual measurements of R/IR may also be made.

### Acknowledgments

We acknowledge financial support from Natural Environment Research Council to S.D. Prince and to J. Silvertown and from the Open University Research Committee to J. Silvertown. At the Open University B. Dick, M. Jarvis, T. King, K. Quick, M. Tremlett and at Queen Mary College B. Frankland, D. Hunt, A. McLellan and P. Wilson contributed significantly to the design and construction of the instrument and its software.

### References

- Deregibus, V.A., Sanchez, R.A., Casal, J.J. & Trlica, M.J. (1985) Tillering responses to enrichment of red light beneath the canopy in a humid natural grassland. *Journal of Applied Ecology*, **22**, 199–206.
- Fenner, M. (1978) A comparison of the abilities of colonizers and closed-turf species to establish from seed in artificial swards. *Journal of Ecology*, **66**, 953–963.
- Frankland, B. (1980) Phytochrome and seed germination. *What's New in Plant Physiology*, **11** (8), 29–32.
- Frankland, B. & Poo, W.K. (1980) Phytochrome control of seed germination in relation to natural shading. In *Photoreceptors and Plant Development* (ed. J. De Greef), pp. 357–366. Antwerpen University Press, Antwerpen, Belgium.
- Gross, K.L. & Werner, P.A. (1982) Colonizing abilities of 'biennial' species in relation to ground cover: implications for their distribution in a successional sere. *Ecology*, **63**, 921–931.
- Holmes, M.G. & Smith, H. (1977) The function of phytochrome in the natural environment 2. The influence of vegetation canopies on the spectral energy distribution of natural daylight. *Photochemistry and Photobiology*, **25**, 539–545.
- Jordan, C.F. (1969) Derivation of Leaf Area Index from quality of light on the forest floor. *Ecology*, **50**, 663–666.
- McConnaughay, K.D.M. & Bazzaz, F.A. (1987) The relationship between gap size and performance of several colonizing annuals. *Ecology*, **68**, 411–416.
- Silvertown, J. (1981) Microspatial heterogeneity and seedling demography in species-rich grassland. *New Phytologist*, **88**, 117–128.
- Silvertown, J. & Wilkin, F.R. (1983) An experimental test of the role of micro-spatial heterogeneity in the co-existence of congeneric plants. *Biological Journal of the Linnean Society*, **19**, 1–8.

- Thompson, K., Grime, J.P. & Mason, G. (1977) Seed germination in response to diurnal fluctuations of temperature. *Nature*, **67**, 147–149.
- Watt, T.A. (1987) The biology and toxicity of ragwort (*Senecio jacobaea* L.) and its herbicidal and biological control. *Herbage Abstracts*, **57**, 1–16.
- Wells, G.J. & Haggard, R.J. (1984) The ingress of *Poa annua* into perennial ryegrass swards. *Grass and Forage Science*, **39**, 297–303.

- Woodward, F.I. (1983) Instruments for the measurement of photosynthetically active radiation and red, far-red and blue light. *Journal of Applied Ecology*, **20**, 103–115.

*Received 6 October 1987; revised 5 January 1988;  
accepted 15 January 1988*